A new approach to modeling the flow curve of hot deformed austenite

Xavier Quelennec, Nathalie Bozzolo, John J. Jonas, Roland E. Logé

A new approach to modeling the flow curve of hot deformed austenite

X. Quelennec[1], N. Bozzolo[2], J.J. Jonas[1], and R. Loge[2]

[1] McGill University, Materials Engineering, 3610 University St, Montréal, Québec, H3A 2B2, Canada

[2] MINES ParisTech, CEMEF - Centre de Mise en Forme des Matériaux, CNRS UMR 7635, BP 207, 06904 Sophia Antipolis Cedex, France

Synopsis

A new, more physically realistic and practically useful model is presented for the simulation of high temperature austenite flow curves. It is an extension of our earlier empirical model based on the Avrami kinetics of dynamic recrystallization. In the new approach, the normalization parameter is expressed in terms of the fractional recrystallization and not the amount of softening. Compression experiments carried out on a Nb-modified plain carbon steel enable the simulated flow curves and progress of recrystallization predicted by the two models to be compared.

1. Introduction

The modeling of austenite flow curves is required for the calculation of separation force and torque in rolling mills[1]. When dynamic recrystallization (DRX) takes place in addition to dynamic recovery during straining, the net softening produced has an influence on these parameters. For this reason, models incorporating Avrami kinetics have been developed[2-4] to take this phenomenon into account. Some authors have defined the amount of DRX softening with respect to the peak stress σ_p[5,6]. Alternatively, the net softening due to DRX can be defined as the difference between the work hardening curve pertaining to the as-yet unrecrystallized grains and the experimental flow curve[7]. The amount of softening can then be normalized so that the kinetics are expressed in terms of the fractional softening[7,8]. Still other models have described the progress of DRX in terms of the volume fraction recrystallized[9].

In the present study, a new method is proposed for quantifying the amount of softening produced by DRX that is expressed in terms of the fractional recrystallization. The previous approach employed a normalization term based on the net softening attainable at large strains. In the present method, softening is described instead in terms of the volume fraction of material that has undergone recrystallization and does not require knowledge of the large strain steady state stress. The modified normalization technique now represents the current state of the material correctly, so that the fractional softening is described in a more physically appropriate manner. It also employs an experimental measure of the stress required to propagate DRX and thus avoids the necessity of extrapolation to estimate the steady state stress or the requirement to carry out experiments to large strains.

Some compression tests were carried out on a Nb-modified plain carbon steel to test the new method. Flow curves derived using the two approaches were then calculated and the results obtained are

compared below.

2. Flow curve modeling

In the previous approach to flow curve modeling, the flow stress pertaining to the as-yet unrecrystallized grains was first derived. From this, the net softening attributable to dynamic recrystallization (DRX) was then calculated[6-8]. This led to equation 1, in which σ_{wh} is the work hardening flow stress, σ_{sat} the saturation value of the work hardening flow curve, σ_{ls} the large strain flow stress of the experimental flow curve, and $X=(\sigma_{wh} - \sigma)/(\sigma_{sat} - \sigma_{ls})$ is the fraction of net softening due to DRX. This will be referred to as the "empirical softening parameter" below.

$$\sigma = \sigma_{wh} - X(\sigma_{sat} - \sigma_{ls}) \tag{1}$$

As long as the strain remains below the critical value for the initiation of DRX, ε_c, the experimental flow stress is defined by the work hardening flow curve. Once ε_c has been exceeded, the softening generated by the activation of DRX, given by $X(\sigma_{sat} - \sigma_{ls})$, must be subtracted from σ_{wh}.

Here the fractional softening X was defined with respect to the net overall softening produced at large strains σ_{sat} - σ_{ls}. When the work hardening flow stress and the experimental flow stress have respectively reached their final values, X was arbitrarily set equal to 1. This method employed the final softening attained at large strains to define the fractional softening at any strain between the critical and final strains. It had the drawback that it describes the state of the material at any time t with regard to a reference state that is present at the end of the test and which, as will be shown below, is in fact microstructurally variable. It also had the drawback that the final state depended on the maximum strain that could be imposed by the testing equipment. For these reasons, a new approach is proposed here, where the fractional softening is defined in terms of the current state of

4

the material and not as a function of σ_{sat} and σ_{ls}.

According to this method, the flow curve can be modeled using a rule of mixtures based on the current values of the work hardening flow stress σ_{wh} pertaining to the unrecrystallized portion of the material and the dynamic recrystallization flow stress $\overline{\sigma}_{rex}$. The latter represents the average flow stress of the remainder of the material, that is, of the grains that have already undergone dynamic recrystallization. This concept is expressed by equations 2a and 2b, where the latter follows the formalism of equation 1 for comparison purposes.

$$\sigma = (1 - X')\sigma_{wh} + X'\overline{\sigma}_{rex} \tag{2a}$$

$$\sigma = \sigma_{wh} - X'\left(\sigma_{wh} - \overline{\sigma}_{rex}\right) \tag{2b}$$

By comparing equations 1 and 2b, it can be seen that the empirical softening term has been replaced by the current value of the difference between the two flow stresses, σ_{wh} - $\overline{\sigma}_{rex}$. For this reason, the previous method described by equation 1 will be referred to here as the "empirical softening parameter method" and the new approach as the "physical softening parameter method". Under these conditions, the new fractional softening X' is defined as follows:

$$X' = \frac{\sigma_{wh} - \sigma}{\sigma_{wh} - \overline{\sigma}_{rex}} \tag{3}$$

Note that the denominator in equation 3 differs from the one applicable to X, which is $\sigma_{sat} - \sigma_{ls}$ (see equation 1).

3. Descriptions of work hardening

In order to use equations 1 and 2 to model flow curves, relations for σ_{wh} and $\overline{\sigma}_{rex}$ must first be derived. For this purpose, work hardening is described by equation 4, which states that the evolution

of the dislocation density ρ with strain only depends on the current value of the dislocation density via the work hardening parameters : r, the rate of dynamic recovery, and h, the athermal work hardening rate[10]. Here, the r and h parameters are taken to be strain independent[7,11].

$$d\rho / d\varepsilon = h - r\rho \tag{4}$$

In order to obtain a general equation describing the work hardening flow curve, equation 4 must be integrated and ρ converted into stress, using the expression $\sigma = M\alpha\mu b\sqrt{(\rho)}$. Here M is the Taylor factor, μ the shear modulus, b the Burgers vector and α a material constant about equal to 0.5. This conversion leads to equation 5, as demonstrated in our previous paper[7].

$$\sigma_{wh} = \left[\sigma_{sat}^2 - \left(\sigma_{sat}^2 - \sigma_0^2\right)exp\left(- r\left(\varepsilon - \varepsilon_0\right)\right)\right]^{1/2} \tag{5}$$

Here σ_{wh} is the work hardening flow stress and σ_0 is the yield stress, at which point $\rho=\rho_0$ and $\varepsilon=\varepsilon_0$. The work hardening flow curve describes the evolution of the flow stress from its value σ_0 at the yield strain ε_0 until it reaches the saturation stress σ_{sat}. It has been shown that σ_{sat} depends on h and r according to[7]:

$$\sigma_{sat} = M\alpha\mu b\sqrt{(h/r)} \tag{6}$$

In the case of $\overline{\sigma}_{rex}$, which represents the work hardening behavior of the grains that have already undergone DRX, its description, given by equation 7, is based on a modification of equation 5, which only applies to the unrecrystallized material. It comes into operation at the critical strain ε_c instead of the yield strain as there is no DRX before this strain. At the critical strain, the flow stress of the first grain to undergo DRX decreases from σ_{wh} to σ_0 (here it is assumed that the effect on the yield stress of the grain size changes brought about by recrystallization can be neglected). For this reason, $\overline{\sigma}_{rex}$ begins with a stress value of σ_0 at the critical strain ε_c. As the strain is increased, the flow stress $\overline{\sigma}_{rex}$ represents a population of grains at later and later stages of the recrystallization process. It finally

6

reaches the saturation value σ_{ss}, considered as the average stress when all the grains have undergone at least one cycle of DRX.

It has been previously demonstrated that, for a broad range of steel grades, the steady state stress is equal to the critical stress for the nucleation of DRX[7]. For this reason, in equation 7, σ_c plays the role of the saturation stress value for $\overline{\sigma}_{rex}$.

$$\overline{\sigma}_{rex} = \left[\sigma_c^2 - \left(\sigma_c^2 - \sigma_0^2\right)exp\left(-r'\left(\varepsilon - \varepsilon_c\right)\right)\right]^{1/2} \tag{7}$$

This is physically reasonable as it signifies that the stress required to continue the propagation of DRX once all the grains have undergone at least one cycle of recrystallization (and have continued to work harden) is the same as the critical stress σ_c that was required to initiate the process in the initial work hardened material.

An experimental flow curve σ_{exp} is displayed in Figure 1, where the values for σ_{wh}, $\overline{\sigma}_{rex}$, σ_0, σ_c, σ_{sat}, σ_{ls} and σ_{ss} are also shown. This diagram reveals the differences between the empirical terms ($\sigma_{sat} - \sigma_{ss}$) and ($\sigma_{sat} - \sigma_{ls}$) and the more physically realistic term ($\sigma_{wh} - \overline{\sigma}_{rex}$). In figure 1, σ_{ls} represents the final flow stress attained in a particular test and σ_{ss} the steady state stress, with $\sigma_{ls}=\sigma_{ss}$ if the latter is reached.

The flow stress $\overline{\sigma}_{rex}$ describes the average state of a mixture of grains, some of which are newly recrystallized and others are recrystallized grains at different stages of being work hardened. As a consequence, the work hardening parameter r' no longer describes the recovery rate alone but also takes into account the appearance of newly recrystallized (and therefore fully softened) grains. Therefore r' differs from the definition of r referred to above. By contrast, h is identical for σ_{wh} and $\overline{\sigma}_{rex}$ on the basis that the intrinsic work hardening rate is the same in recrystallized and not yet recrystallized grains. The relation between σ_c, h and r' is given by equation 8.

7

$$\sigma_c = M\alpha\mu b\sqrt{(h/r')} \tag{8}$$

In order to model flow curves and compare the predictions of the "empirical softening parameter method" and the "physical softening parameter method", the values of X and X´ have to be calculated as a function of the Zener-Hollomon parameter $Z = \dot{\varepsilon}\exp(Q_{def}/RT)$, where $\dot{\varepsilon}$ is the strain rate, Q_{def} the activation energy of the deformation, and R the gas constant. For X and X´, the Avrami formalism is used here to describe the kinetics of DRX[7]. This is given by equations 9 and 10 below, where t is the time during which dynamic recrystallization has been operating, k is the Avrami constant, and n the Avrami time exponent. Thus, only the dependences of n and k on Z are needed to describe X (n´ and k´ for X´).

$$X = 1 - \exp(-kt^n) \tag{9}$$

$$\log\ln[1/(1-X)] = \log k + n\log t \tag{10}$$

4. Experimental procedure

Flow curve modeling requires that the experimental dependences on Z of the following quantities must first be established: i) σ_0, σ_c, σ_{sat}, r', n' and k' for the present approach; and ii) σ_0, σ_c, σ_{ls}, σ_{sat}, r, n and k for the previous method. In the present example, a Nb-modified plain carbon steel, of which the composition is C 0.11, Si 0.26, Mn 1.1, Nb 0.038, S 0.003, P 0.004, O 0.004, Al 0.03, N 0.003 (wt%), was tested in compression. The deformation conditions used are listed in Table1. Cylindrical compression samples (11.4 mm in height and 7.6mm in diameter) were machined from rolled plates with the cylinder axes parallel to the rolling direction. Grooves were machined into the end faces of the samples in order to provide reservoirs for the boron nitride lubricant that was employed. Constant strain rate compression testing was carried out on an MTS servo-hydraulic

machine with a maximum load capacity of 100 kN. Samples were heated up to 1200°C and held for 15 minutes and then cooled to the deformation temperature. The specimens were held for 5 minutes at temperature to permit homogenization prior to testing.

5. Experimental flow curves

A selection of stress-strain curves is presented in Figure 2-a. At 1200°C, these curves exhibit well defined peaks and steady state stresses typical of the occurrence of dynamic recrystallization[12]. Conversely, no peaks were observed at the lowest temperature (T=950°C) in the range of strain rates studied. The deformation activation energy Q_{def} was determined from the peak or maximum stresses and a value of 351 kJ.mol^{-1} was obtained; the latter is in good agreement with those reported by previous workers[2,3].

The yield stresses were defined using a 2 % offset. The part of each flow curve between 'yielding' and ε_c was fitted with a 7th order polynomial using the MATLAB^{TM} software. The critical stresses and strains associated with the initiation of DRX were calculated by means of the double differentiation method[13].

The difference between the large strain stress σ_{ls} and the critical stress σ_c is highlighted in Figure 2-b. At low Z values, $\sigma_c = \sigma_{ls}$, as observed in other steels[7], which means that the steady state stress σ_{ss} has been reached. As Z is increased σ_{ls} deviates more and more from σ_c. These deviations are taken here to signify that, under relatively high Z conditions, the extent to which DRX has propagated through the microstructure at a given strain decreases with increasing Z.

6. Modeling results

To calculate σ_{wh}, the parameters h and r were derived using the procedure described in our earlier

9

paper[7]. This involved replotting the stress-strain data in the form of $2\theta\sigma$ vs. σ^2 curves, with θ the

strain hardening rate. As long as this plot is linear, r is obtained from the slope while σ_{sat} can be

determined from the vertical intercept $r\sigma_{sat}^2$. Then h in turn is calculated from h=r $[\sigma_{sat}/(M\alpha\mu b)]^2$

(equation 6).The temperature dependences of b[14] and μ[15] were taken into account and M and α were

set equal to 3 and 0.5[16], respectively. For the description of $\overline{\sigma}_{rex}$, r´ was calculated using equation 8,

as h and σ_c are known.

A set of $2\theta\sigma$ vs. σ^2 plots derived in this way is illustrated in Figure 3-a and the values of r and r´

obtained are displayed in Figure 3-b as functions of Z. Each pair of r-r´ values characterizes a single

experimental flow curve.

With the aid of these quantities, the σ_{wh} and $\overline{\sigma}_{rex}$ flow curves were constructed for each set of

experimental conditions. Then, values of $X(\varepsilon)$ and $X´(\varepsilon)$ were determined from each experimental

curve using equations 1 and 3, examples of which are shown in Figure 4. The Avrami kinetics (X and

X´) were determined for each experimental condition using equation 10 and the parameters n, n´, k

and k´ were derived from these plots as described above.

The dependences of σ_0, σ_c, σ_{sat}, r', n' and k' on Z, used for the "physical softening parameter

model", are described by equations 11 to 16. The stress dependences are displayed in Figure 5-a. The

dependences of σ_0, σ_c, σ_{ls}, σ_{sat}, r, n and k on Z, used for the "empirical softening parameter model",

are described by equations 11 to13 plus 17 to 20. In this case, the stress dependences are displayed in

Figure 5-b. It should be noted that the peak stress σ_p is not employed in either treatment.

$$\sigma_0 = 15.7*log(Z)-157 \tag{11}$$

$$\sigma_c = 29.7*log(Z)-309 \tag{12}$$

$$\sigma_{sat} = 32.7*log(Z)-327 \tag{13}$$

$$r' = 6 + 2.5 * 10^6 Z^{-0.5} \tag{14}$$

$$n' = 29.7 * Z^{-0.081} \tag{15}$$

$$k' = \frac{-\ln(0.5)}{(9.3 * 10^{21} * T^{-7.3} * \dot{\varepsilon}^{-0.7})^{n'}} \tag{16}$$

$$\sigma_{ls} = 32.7 * log(Z) - 327 \\ - exp(-3 * 10^{-10} Z^{0.7})[3 * log(Z) - 18] \tag{17}$$

$$r = 4 + 9.6 * 10^5 Z^{-0.5} \tag{18}$$

$$n = 9 * Z^{-0.037} \tag{19}$$

$$k = \frac{-\ln(0.5)}{(1.3 * 10^7 * T^{-2.5} * \dot{\varepsilon}^{-0.9})^{n}} \tag{20}$$

The above equations (11 to 20) are only applicable to the present Nb steel and their equivalents must be determined experimentally for each new composition of interest. As examples, the effects on the Avrami kinetics of adding Mo and Nb to a plain C steel are illustrated in Figure 6. These data are described in more detail in ref. 17. It is evident from this diagram that, at 1000°C, the t_{50}'s for DRX are 2.34, 2.75 and 3.46 for the plain C, Mo and Nb steels, respectively. Thus the addition of the latter two elements to a plain C steel retards the rate of DRX by ratios of 1.17 and 1.48, respectively. The predictions of the two methods are compared in Figure 7 for T=1050°C and four strain rates

($\dot{\varepsilon}$ =0.05s^{-1}, 0.1s^{-1}, 0.25s^{-1} and 0.5s^{-1}). The results displayed in this diagram show that the "empirical softening parameter method" and the "physical softening parameter method" lead to similar flow curves. However, there are important differences in the strain (time) dependences of X and X' (see Figure 4).While both adequately specify the progress of mechanical softening, X' provides a reasonable description of the volume fraction recrystallized as well. By contrast, X does not. This

11

difference is examined in more detail below.

7. Fractional softening and volume fraction recrystallized

As shown in Figure 4-b, cases arise where X' approaches its asymptotic value of 1 significantly more slowly than X. This corresponds to the case where the $\overline{\sigma}_{rex}$ flow curve has not yet reached its asymptotic value of σ_c at the maximum strain attainable in a given test. Under these conditions, the final flow stress σ_{ls} is greater than the critical stress σ_c (Figure 2-b). This difference increases with Z; in a corresponding manner, the final value of X' decreases. This signifies that DRX is less and less capable of propagating through the material (per unit strain) as Z is increased.

Important support for this interpretation is provided by the plots of the values of the fractional softening X and X' calculated at the peak strain and displayed in Figure 8. Here it can be seen that the peak strain value of X' takes a constant value of 0.125 that is independent of Z when calculated by the "physical softening parameter method". This is physically appropriate as the peak strain represents the stage in the DRX process at which the softening effects of DRX exactly match the hardening effects in the unrecrystallized material. By contrast, with the empirical method, "full softening" (X=1) is associated with a variable amount of fractional recrystallization, i.e. with a range of values of σ_{ls} - σ_c where the latter difference is zero when DRX has propagated completely through the material. Conversely, at the peak strain, where the volume fraction recrystallized can be assumed to be constant, X can take a range of values (Figure 8) depending again on the extent to which σ_{ls} has approached its asymptotic value $\sigma_{ss} = \sigma_c$. Thus it can be seen that according to the "physical softening parameter method" the fractional softening has a direct interpretation as a measure of the recrystallized volume fraction. In addition, the final stress on a stress-strain curve is a straightforward

measure of this fraction in that X' equals zero when $\sigma_{ls}=\sigma_{sat}$ and one when $\sigma_{ls}=\sigma_c$.

Numerous results have shown that DRX can be initiated under many thermomechanical processing conditions, but the present approach confirms that DRX is slower at high Z, that is, it is less able to propagate through the material per unit strain. This leads to situations where the critical stress σ_c and strain ε_c are attained, but the flow curve does not exhibit a distinct peak or any significant softening (Figure 3-a). Experiments are currently under way in materials that do not undergo a phase change during quenching to examine the relationship between softening and fractional recrystallization[19]. These results will be reported in a separated publication.

8. Conclusions

A new way to calculate the flow curve of hot deformed austenite has been proposed. This requires a definition of the mean flow stress of the dynamically recrystallized material. The new approach provides a physically more realistic description of DRX than our earlier empirical model, which was limited to the quantification of the amount of mechanical softening, but did not address the question of the volume fraction recrystallized. The simulated flow curves generated by the new "physical softening parameter method" were compared with those obtained from the previous "empirical softening parameter method" for a Nb-modified plain carbon steel. It is evident that the two approaches lead to similar flow curves, but the new method provides a description of the volume fraction recrystallized while the earlier approach does not.

A significant advantage of the new method is that it only requires knowledge of the Z-dependences of the yield stress σ_0 and critical stress σ_c for the initiation of DRX. In addition, the Z-dependences of the Avrami coefficients must also be known, which can be readily determined from the differences

between the work hardening σ_{wh} and experimental σ flow stresses.

References

(1) P. Hodgson, J.J. Jonas and C.H.J. Davies: Handbook of Thermal Process Modeling of Steels, ed. by C. Hakan Gür and J. Pan, CRC Press, Taylor & Francis Group, (2009), 225.

(2) A.I. Fernández, P. Uranga, B. Lopez and J.M. Rodriguez-Ibabe: Mater. Sci. & Engin., A361(2003), 367.

(3) L. Ma, Z. Liu, S. Jiao, X. Yuan and D. Wu: J. Iron & Steel Res. Int., 15(2008), 31.

(4) J. Wang, J. Chen, Z. Zhao and X. Ruan: J. Iron & Steel Res. Int., 15(2008), 78.

(5) S. Serajzadeh and A. Karimi Taheri: Materials & Design, 23(2002), 271.

(6) M. El Wahabi, L. Gavard, F. Montheillet, J.M. Cabrera and J.M. Prado: Acta Mater., 53(2005), 4605.

(7) J.J. Jonas, X. Quelennec, L. Jiang and E. Martin: Acta Mater., 57(2009), 2748.

(8) H. Mirzadeh and A. Najafizadeh: Materials & Design, 31(2010), 4577.

(9) G.R. Stewart, A.M. Elwazri, S. Yue and J.J. Jonas: Mater. Sci. & Techn., 22(2006), 519.

(10) Y. Estrin and H. Mecking: Acta Metall., 32(1984), 57.

(11) A. Laasraoui and J.J. Jonas: Metall. Trans., A22(1991), 1545.

(12) T. Sakai and J.J. Jonas: Acta Metall., 32(1984), 198.

(13) E.I. Poliak and J.J. Jonas: Acta Mater., 44(1996), 127.

(14) I. Seki and K. Nagata: ISIJ Int., 45(2006), 1789.

(15) G. Ghosh and G.B. Olson: Acta Mater., 50(2002), 2655.

(16) B. Reichert and Y. Estrin: Steel Res. Int., 78(2007), 791.

(17) X. Quelennec, E. Martin, L. Jiang and J.J. Jonas: Proc. of 15th Int. Conf. on the Strength of Materials, J. Phys.: Conference Series (JPCS), 240(2010), 012082.

(18) C. Yue, L. Zhang, S. Liao, J. Pei, H. Gao, Y. Jia and X. Lian: Mater. Sci. Eng., A499(2009), 177.

(19) S. Rouselle, R. Loge and N. Bozzolo, to be published

List of Tables

Table 1: Deformation parameters pertaining to the steel tested.

Figure captions

Figure 1: Schematic diagram of an experimental flow curve σ_{exp} and the derived work hardening σ_{wh} and recrystallization $\overline{\sigma}_{rex}$ flow curves. The dependences on strain of the numerators in the definitions of X and X' are also shown.

Figure 2: a) Experimental flow curves determined on the present Nb-modified plain carbon steel. The curves for 1000, 1075 and 1150°C are not displayed here. b) σ_{ls} and σ_c data determined on the present steel. The data are compared to a line representing $\sigma_{ls} = \sigma_c$.

Figure 3: a) Selected $2\theta\sigma$ vs. σ^2 plots derived from the compression curves of Figure 2. The critical stresses σ_c are represented by open circles and the linear regimes by dashed lines. b) Dependences of the work hardening parameters r and r´ on Z, the Zener-Hollomon parameter.

Figure 4: Values of fractional softening X and X´ calculated for the following experimental conditions: a) T=1150°C and $\dot{\varepsilon}$ =0.25s^{-1}, b) T=1050°C and $\dot{\varepsilon}$ =0.25s^{-1}

Figure 5: a) Dependences of σ_0, σ_c and σ_{sat} on Z. b) Dependences of σ_0, σ_c, σ_{ls} and σ_{sat} on Z.

Figure 6: Avrami plots calculated for T=1000°C and $\dot{\varepsilon}$ =0.1s^{-1} for 3 steels (a plain C steel[3] (labelled A), a Mo high C steel[18] (labelled B) and a Nb low C steel[3] (labelled C)) showing the effects of adding Mo and Nb to a plain C steel.

Figure 7: Comparison of the simulated flow curves derived using the "empirical" and "physical" softening parameter methods.

Figure 8: Dependences on Z of the fractional softening values X and X´ calculated at the peak strain.

Table

Table1

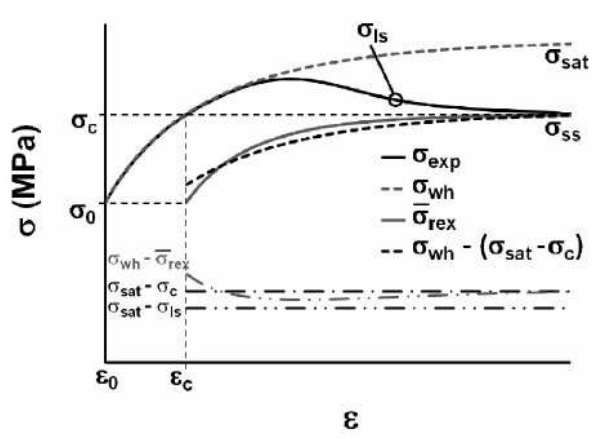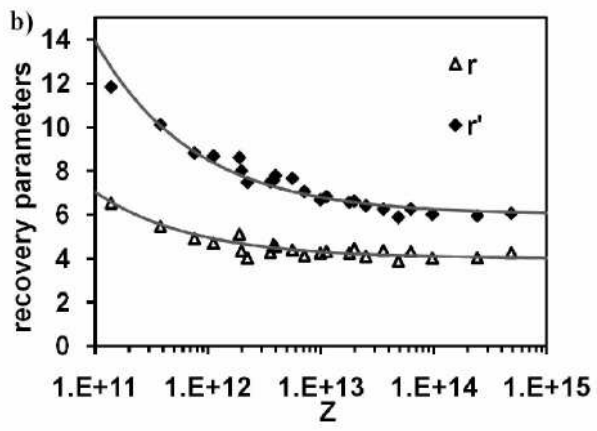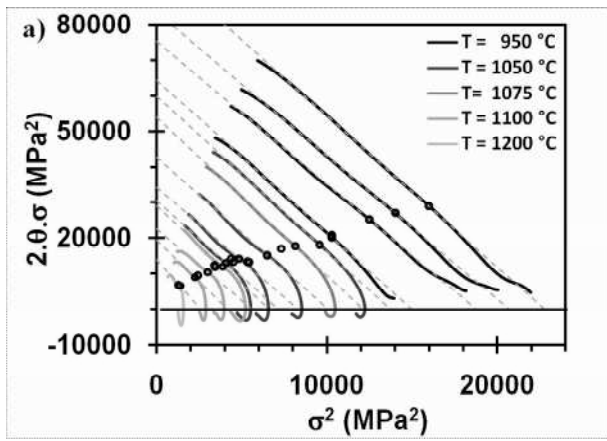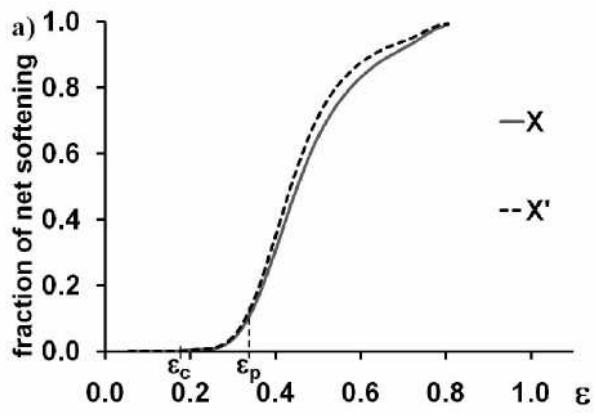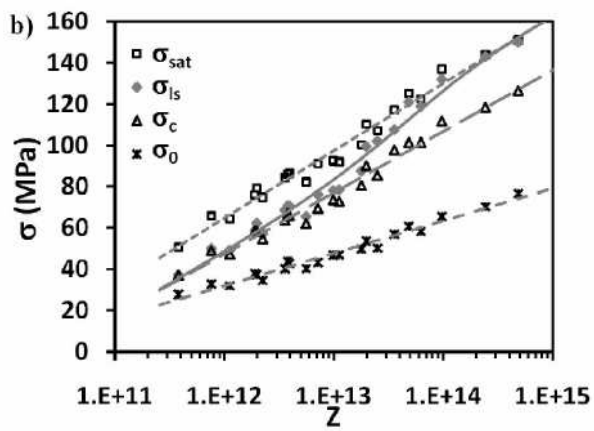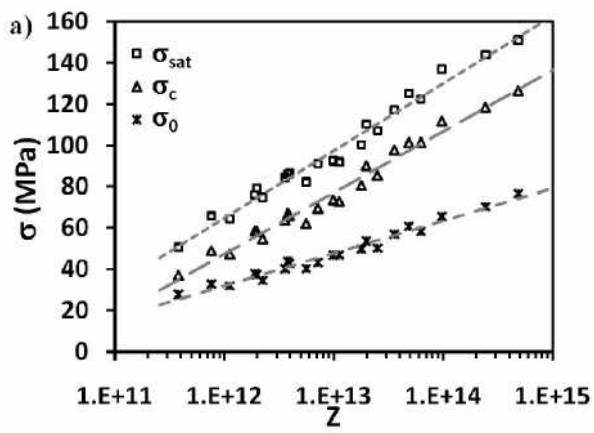| T (°C)	$\dot{\varepsilon}$ (s^{-1})
950	0.5, 0.25, 0.1, 0.05
1000	0.1, 0.25
1050, 1075, 1100, 1150	0.5, 0.25, 0.1, 0.05
1200	0.05

Figures

Figure 1

Figure 2
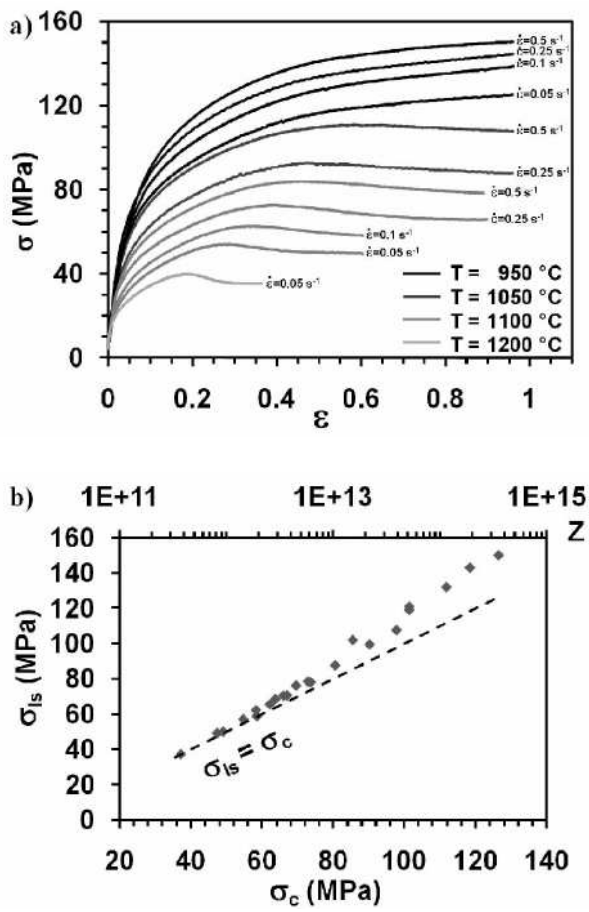
Figure 3

Figure 4
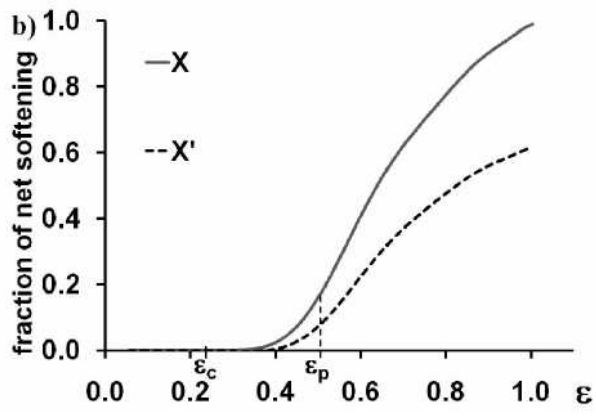
Figure 5

Figure 6

Figure 7

Figure 8